Biophysical Chemistry 41 (1991) 101–110
Elsevier Science Publishers B.V., Amsterdam

BIOCHE 01608

Charge formation in microporous membranes by single-acid site dissociation

H.J.M. Hijnen and J.A.M. Smit *

Gorlaeus Laboratories of the State University of Leiden, P.O. Box 9502, 2300 RA Leiden (Netherlands)

Abstract

The electrolyte concentration and pH dependence of the effective charge density of weak ion exchange membranes have been studied by combining solutions of the Poisson–Boltzmann equation in cylindrical pores with a simple dissociation equilibrium of weakly acid groups attached to the pore walls. Analytical expressions for the effective charge density and wall potential are presented which describe these quantities in terms of pH, electrolyte (1 : 1) concentration, acid constant, density of acid groups and the pore size. The concentration dependence of the effective fixed charge density experimentally observed for cellulose membranes and NaCl-solutions agrees quantitatively with the theoretical predictions. For track-etched mica membranes and KCl-solutions the influence of pH and electrolyte concentration on the effective charge density can be qualitatively explained. Also an interpretation of electro-osmotic findings obtained with an asymmetric cellulose acetate membrane and NaCl-solutions is given.

Keywords: Polyelectrolytes; Charge formation; Electro-osmotic effects; Microporous membranes; Poisson–Boltzmann equation

1. Introduction

Charge formation at surfaces has grown for many years to an important area in the study of colloidal particles [1,2]. Charges may be formed by ionization of functional groups attached at the surfaces. For instance in the case of carboxyl groups the number of COO^- groups will increase with increasing pH by protolysis. On the other hand protons will bind to the negatively charged surface when the pH is decreased. The equilibrium state can be described by a surface dissociation constant K_a which follows from the familiar mass action law. It has become practice to combine the description of this simple dissociation equilibrium with the double layer theory. In this approach the relationship between charge density and potential at the surface is in principle given by the Poisson–Boltzmann (PB) equation. A review has been given by Healy and White [3] treating a number of cases according to the Gouy–Chapman model of the electrical double layer and using the flat plate approach solution of the Poisson–Boltzmann equation. For colloidal particles it has become custom to introduce two regions, i.e. the diffuse double layer, in which the variation of the electrostatic potential is described by the PB-equation, and a Stern layer, which accounts for the finite size of the ions and for the solvent properties in the direct neighbourhood of the surface.

Obviously also at charged membrane surfaces charge formation phenomena of the same type as

* To whom correspondence should be addressed.

0301-4622/91/$03.50

mentioned above will play a part. In this paper we study charge formation in a charged cylindrical pore. The capillary may be considered as an elementary unit of a membrane which is thought to be composed of a bundle of parallel pores. We show that for small pores the curvature cannot be neglected and consequently the flat plate solution of the PB-equation has to be replaced by the corresponding solution within a cylindrical pore. For simplicity we describe the properties of the electrical double layer within the framework of the Gouy–Chapman model. This model is then combined with a simple (acid) site dissociation model. The theoretical results are presented as relationships for the surface charge density and the surface potential in which the pK_a, pH, electrolyte concentration, density of acid groups and the pore radius as parameters appear. The theory predicts the electrolyte concentration dependence and the pH dependence of the charge density in charged micropores. This is shown for experimental results obtained with cellulose (acetate) [4,5] and track-etched mica membranes [6,7].

2. Theoretical

2.1 Relationships between surface charge density and wall potential resulting from the PB-equation

A charged porous membrane is considered to be in contact with an aqueous electrolyte solution containing counterions ($i = 1$), coions ($i = 2$), protons ($i = 3$) and hydroxide ions ($i = 4$). Electroneutrality in the external solution demands that

$$\sum_i C_{i0} z_i = 0 \tag{1}$$

in which C_{i0} and z_i are respectively the concentration and valence of ion i.

From the dissociation equilibrium of water (dissociation constant K_w) a relation between the concentrations of H^+ (C_{30}) and OH^- (C_{40}) exists

$$C_{30} C_{40} = K_w \tag{2}$$

The membrane is modelled by a bundle of parallel cylindrical capillaries with radius a. Due to the presence of weakly ionizing acid groups, N mol per cm^2, the pore wall is negatively charged. Hence the absolute value of the effective charge density of the capillary q^* is always smaller than NF (F is the Faraday constant, i.e. $F = 2.892599 \times 10^{14}$ e.s.u. mol).

In accordance with the Gouy–Chapman model the mobile ions are assumed to be point charges obeying Boltzmann's distribution law from the pore wall ($r = a$) to the center ($r = 0$). Also a uniform dielectric constant is assumed, mostly $\varepsilon = 78$. Then the Poisson equation for the potential within the pore (ψ) can be written as

$$\frac{1}{r}\frac{\partial}{\partial r} r \frac{\partial \tilde{\psi}}{\partial r} = \frac{4\pi z_1 F}{\varepsilon RT} \sum_i C_i z_i F \tag{3}$$

in which the dimensionless potential $\tilde{\psi}$ is defined as $\tilde{\psi} = -z_1 F\psi/RT$.

Local equilibrium in radial direction leads to a Boltzmann distribution of ions

$$C_i = C_{i0} \exp(z_i/z_1)\tilde{\psi} \tag{4}$$

where C_{i0} is the ion concentration in regions where the potential is defined to be zero [8].

Substitution of eq. (4) in (3) results in the Poisson–Boltzmann (PB) equation within a cylindrical pore.

From the condition of global electroneutrality within the pore it follows that

$$\frac{1}{a}\int_0^a \sum_i C_i z_i F r \, dr = q^* \tag{5}$$

Integrating eq. (3) from $r = 0$ to $r = a$ and using eq. (5) we have the boundary condition

$$\left.\frac{\partial \tilde{\psi}}{\partial r}\right|_{r=a} = 4\alpha/a \tag{6a}$$

in which α is defined as

$$\alpha = \frac{\pi F |z_1| q^* a}{\varepsilon RT} \tag{6b}$$

The integrated PB-equation yields a relation between q^* and $\tilde{\psi}_w$. In the following we treat three types of analytical approaches which are valid in specific regimes.

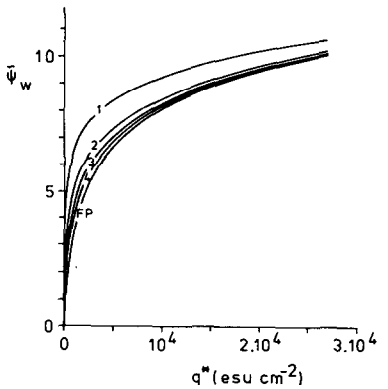

Fig. 1. Effect of the pore radius on the relationship between dimensionless wall potential and effective charge density. $\varepsilon = 78$; $T = 298$ K; $c = 10^{-7}$ mol cm^{-3} (1:1 electrolyte); pH = 5.7 CE-curves 1–4: eq. (7) with (1), $a = 10^{-7}$ cm; (2), $a = 5 \times 10^{-7}$ cm; (3), $a = 10^{-6}$ cm; (4), $a = 2 \times 10^{-6}$ cm. FP-curve: eq. (9b).

For concentrations small enough to ensure that even in the center of the pore $\tilde{\psi}$ is larger than 1, the contribution of the coions in eq. (3) can be neglected. In this so-called coion exclusion regime (CE) we have for 1:1 electrolytes [9]

$$\tilde{\psi}(r) = \ln \frac{16\alpha(1+\alpha)}{(\lambda a)^2\{1+\alpha-\alpha(r/a)^2\}^2},$$

$$\tilde{\psi}(0) \geq 1 \tag{7}$$

with λ defined by $\lambda^2 = 8\pi F^2(C_{10} + C_{30})/\varepsilon RT$. Specifying eq. (7) to $r = a$ and using eq. (6b) we arrive after some rearranging at

$$q^* = \frac{4(C_{10} + C_{30})F}{\lambda} \times \left[\left\{\tfrac{1}{4}\exp\tilde{\psi}_w + (\lambda a)^{-2}\right\}^{1/2} - (\lambda a)^{-1}\right] \tag{8}$$

Plots according to this equation are shown in Fig. 1 for a 1:1 electrolyte with $C_{10} = 10^{-7}$ mol cm^{-3}, pH = 5.7 ($C_{30} = 2.0 \times 10^{-9}$ mol cm^{-3}) and varying values of the pore radius. It can be observed that above $a = 10^{-6}$ cm (10 nm) the influence of the pore radius on the curves becomes vanishingly small. The limiting curve in Fig. 1 (FP) is given by the flat plate expression [1]

$$(q^*)^2 = \frac{\varepsilon RT}{2\pi}\sum_i C_{i0}\{e^{(z_i/z_1)\tilde{\psi}_w} - 1\} \tag{9a}$$

which in the case of a 1:1 electrolyte reduces to

$$q^* = \frac{4(C_{10} + C_{30})F}{\lambda}\sinh(\tilde{\psi}_w/2) \tag{9b}$$

For large pore radii eqs. (9) are expected to be valid over the whole salt concentration range.

Still another approximative solution of the PB-equation, valid over the whole salt concentration range but restricted to rather flat potential profiles within the pore, is of interest. This so-called [10] spatial averaging solution (SA) is a reasonable approximation as long as deviations from the average dimensionless potential ($\bar{\tilde{\psi}}$), defined by

$$\bar{\tilde{\psi}} = \frac{2}{a^2}\int_0^a \tilde{\psi} r \, dr \tag{10}$$

are smaller than unity for every value of r, which in fact implies $\tilde{\psi}_w - \bar{\tilde{\psi}} \leq 1$. In that case we have the solution

$$\tilde{\psi}(r) = \bar{\tilde{\psi}} + \frac{8\alpha}{Ha}\left\{\frac{I_0(Hr)}{2I_1(Ha)} - \frac{1}{Ha}\right\} \tag{11}$$

in which H is defined by $H^2 = (4\pi F^2/\varepsilon RT)\sum_i C_{i0}(z_i)^2 e^{(z_i/z_1)\bar{\tilde{\psi}}}$. I_0 and I_1 are modified Bessel functions of resp. the zeroth and first order. The average potential can be derived from eq. (5)

$$q^* = (a/2)\sum_i C_{i0} z_i F e^{(z_i/z_1)\bar{\tilde{\psi}}} \tag{12a}$$

which for 1:1 electrolytes reduces to

$$q^* = aF(C_{10} + C_{30})\sinh\bar{\tilde{\psi}} \tag{12b}$$

The range of validity of eqs. (11) to (12) can be estimated for 1:1 electrolytes by elaborating the inequality $\tilde{\psi}_w - \bar{\tilde{\psi}} \leq 1$ in the CE-regime. It turns out that $\alpha \leq 1.4$. Since deviations from the average potential are most markedly at small salt concentrations we may safely assume that the SA-equations are a good approximation over the whole concentration-range provided that $\alpha \leq 1.4$ [11].

2.2 Charge formation by protolysis

If weakly acid groups are attached to the pore wall, protons may dissociate from these groups,

whereas a negatively charged surface is left behind. Following the approach of a simple dissociation equilibrium at the surface [2,3]

$$AH \rightleftarrows A^- + H^+$$

we define the dissociation constant K_a under the assumption of ideal solutions by

$$K_a = \frac{[A^-]}{[AH]} C_{30} \exp(\tilde{\psi}_w) = \frac{f}{1-f} C_{30} \exp(\tilde{\psi}_w) \tag{13}$$

in which the proton activity at the wall is given by eq. (4) specified to $r = a$ and $[A^-]$ and [AH] are surface concentrations. The fraction of acid groups which are actually ionized is denoted by f and is equal to $[A^-]N^{-1}$. The charges formed in this way are supposed to be smeared out over the wall surface. This implies that the absolute value of the effective charge density becomes

$$q^* = fNF \tag{14}$$

Now eq. (13) is easily transformed to

$$\frac{\tilde{\psi}_w}{2.303} - {}^{10}\log(f^{-1} - 1) = \text{pH} - \text{p}K_a \tag{15}$$

This equation can be combined with eq. (14) and solved with respectively eqs. (9b), (8) and (12b) for either $\tilde{\psi}_w$ or f.

In the flat plate (FP) approximation (for large pores) we get

$$\frac{\tilde{\psi}_w}{2.303} - {}^{10}\log\left\{\frac{\xi}{\sinh(\tilde{\psi}_w/2)} - 1\right\} = \text{pH-p}K_a \tag{16}$$

and (FP)

$$2\,{}^{10}\log\left\{f\xi + \left[(f\xi)^2 + 1\right]^{1/2}\right\} - \log(f^{-1} - 1) = \text{pH} - \text{p}K_a \tag{17}$$

in which the parameter ξ is defined by

$$\xi = \frac{\lambda N}{4(C_{10} + C_{30})} \tag{18}$$

Equations similar to eqs. (16) and (18) can be found in literature [2,3].

For the CE-approximation (high potentials or small concentrations) we derive analogously

$$\frac{\tilde{\psi}_w}{2.303} - {}^{10}\log\left\{\frac{(\lambda a\xi)}{\left[\frac{1}{4}(\lambda a)^2 \exp(\tilde{\psi}_w) + 1\right]^{1/2} - 1} - 1\right\} = \text{pH} - \text{p}K_a \tag{19}$$

and (CE)

$${}^{10}\log\left\{\frac{8\xi f}{\lambda a}(1 + \lambda a\xi f/2)\right\} - {}^{10}\log(f^{-1} - 1) = \text{pH} - \text{p}K_a \tag{20}$$

In the SA-approach (flat potential profiles) we find first an equation for $\bar{\tilde{\psi}}$

$$\frac{1}{2.303}\left[\bar{\tilde{\psi}} + \text{tgh}(\bar{\tilde{\psi}})\left\{\frac{Ha}{2}\frac{I_0(Ha)}{I_1(Ha)} - 1\right\}\right] - {}^{10}\log\left\{\frac{4\xi}{\lambda a \sinh(\bar{\tilde{\psi}})} - 1\right\} = \text{pH} - \text{p}K_a \tag{21}$$

in which $H^2 = \lambda^2 \cosh(\bar{\tilde{\psi}})$ (SA)

Once $\bar{\tilde{\psi}}$ is known, $\tilde{\psi}_w$ is given by the first term of the left hand side of eq. (21) which is $\tilde{\psi}_w/2.303$. On the other hand f can be solved using the relation

$$f = \frac{\lambda a}{4\xi} \sinh(\bar{\tilde{\psi}}) \tag{22}$$

which immediately follows from eqs. (12b), (14) and (18).

Equations (16) to (22) enable us to calculate $\tilde{\psi}_w$ and f as a function of the pH and the electrolyte concentration for preset values of N and K_a. The concentration dependences are embedded in ξ ($\sim (C_{10} + C_{30})^{-1/2}$) and λ ($\sim (C_{10} + C_{30})^{1/2}$). Note that the combination $\lambda a\xi$ is independent of $(C_{10} + C_{30})$.

2.3 Relationships with experimentally accessible quantities

Quantities from which q^* can be determined without the complication of requiring additional

information about the diffusion coefficients of the ions within the capillary, are the salt distribution coefficient and the electro-osmotic coefficient (l_{ep}) in combination with the electrical resistance (R_e) and hydrodynamical permeability (L_p) per unit of membrane surface. Measurement of the salt distribution coefficient is carried out under equilibrium conditions. In the determination of the electro-osmotic coefficient, however, a pressure difference (Δp) is applied across the membrane and the resulting potential difference ($\Delta\phi$) is measured.

Under the experimentally applied conditions of equal concentrations on both sides of the membrane ($\Delta c = 0$) and the absence of an electrical current ($I = 0$) the following expression for l_{ep} can be derived (eqs. (18) and (28) of ref. [8])

$$l_{ep} = -\left(\frac{\Delta\phi}{\Delta p}\right)_{I=0;\,\Delta c=0} = \frac{2\varepsilon RT}{\pi z_1 F}\left\{\left(\tilde{\psi}_w - \bar{\tilde{\psi}}\right)/a^2\right\}\frac{l_{11}}{l_{33}} \tag{23}$$

in which l_{11} and l_{33} are respectively the hydrodynamical permeability ($\Delta c = 0$; $\Delta\phi = 0$) and electrical conductivity ($\Delta c = 0$; $\Delta p = 0$) of the capillary.

The ratio l_{11}/l_{33} reads in terms of L_p and R_e

$$\frac{l_{11}}{l_{33}} = L_p R_e \tag{24}$$

Since l_{ep}, L_p and R_e can be determined experimentally, information on $(\tilde{\psi}_w - \bar{\tilde{\psi}})/a^2$ can be obtained by using eqs. (23) and (24). Then, provided that the pore radius is known, the effective charge density can be calculated by applying the solution of the PB-equation. As an example we take the SA-solution, eq. (11), specified to $r = a$

$$\tilde{\psi}_w - \bar{\tilde{\psi}} = \frac{8\alpha}{Ha}\left\{\frac{I_0(Ha)}{2I_1(Ha)} - \frac{1}{Ha}\right\} \tag{25}$$

From eq. (6b) it can immediately be seen that α is a function of q^* and a. The parameter Ha depends on a and $\bar{\tilde{\psi}}$ and is correspondingly (eq. 12a) also a function of q^* and a.

For very narrow capillaries, i.e. $Ha \ll 1$, it is allowed to expand the Bessel functions of eq. (25), which leads to

$$\tilde{\psi}_w - \bar{\tilde{\psi}} = \alpha = \frac{\pi|z_1|F^2}{2\varepsilon RT} C^* a^2 \tag{26}$$

in which C^* is the effective fixed charge concentration defined by

$$C^* = 2q^*/aF \tag{27}$$

The last member of eq. (26) is obtained by substituting eq. (27) in eq. (6b). Combination of eqs. (23), (24) and (26) yields

$$l_{ep} = \frac{|z_1|}{z_1} C^* F L_p R_e \tag{28}$$

Equation (28), known as Schmid's equation, has been used by Demisch and Pusch [5] for the calculation of the effective fixed charge concentration of an asymmetric cellulose acetate membrane from the experimental data.

3. Results and discussion

In the following we shall consider in particular the fraction f which has the meaning of a normalized charge density according to eq. (14). As a consequence of the dissociation equilibrium changes in f are directly coupled to changes in $\tilde{\psi}_w$ provided that pH and pK_a remain constant (eq. 15). If the electrolyte concentration increases in the system (decreasing ξ) the fixed charges are better screened and the dissociation of protons will be enhanced, i.e. f increases. According to eq. (15) this increase is necessarily attended by a decrease of $\tilde{\psi}_w$. Thus $\tilde{\psi}_w$ decreases with decreasing ξ by the screening effect that is only partly compensated by a greater number of dissociated groups. This behaviour is described by means of the eqs. (16), (19) or (21). Conversely eq. (15) dictates that $\tilde{\psi}_w$ shall never be constant with increasing electrolyte concentration which is sometimes adopted as a boundary condition to the PB-equation but obviously not realized by the single-site dissociation mechanism.

Grafically the concentration dependence of f is shown in Fig. 2 (c in Fig. 2 is the concentration of added electrolyte equal to C_{10} for pH < 7 and to C_{20} for pH > 7). Two values for K_a are taken into consideration, $K_a = 10^{-8}$ mol cm^{-3}, a value characteristic for carboxyl groups, and $K_a = 10^{-6}$ mol cm^{-3}. The FP-curves reflect the concentration de-

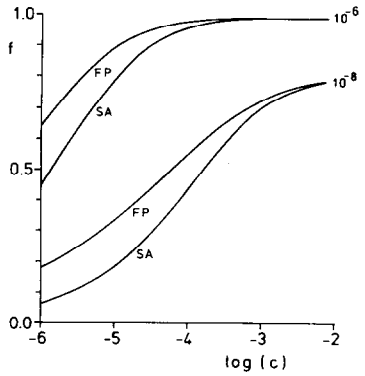

Fig. 2. Concentration dependence of f for two K_a-values, $K_a = 10^{-8}$ mol cm^{-3} and 10^{-6} mol cm^{-3} and with c in mol cm^{-3}. $\varepsilon = 78$; $T = 298$ K; 1:1 electrolytes: pH = 5.7; $N = 5 \times 10^{-11}$ mol cm^{-2}. FP-curve: eq. (17); SA-curve ($a = 10^{-7}$ cm): eqs. (21) and (22).

pendence of f for very large pores whereas the SA-curves represent a similar behaviour for a narrow capillary with pore radius 10^{-7} cm (1 nm). For both values of K_a, f increases strongly with increasing concentration.

With respect to the effect of the pore radius it can be seen from Fig. 2 that f increases with increasing pore size. The influence of the pore radius can be studied in still more detail by applying the CE-expression, eq. (20). In Fig. 3 the results are shown for $c = 10^{-7}$ mol cm^{-3}, $K_a = 10^{-8}$ mol cm^{-3} and two values of N, i.e. $N = 10^{-11}$ mol cm^{-2} and $N = 5 \times 10^{-11}$ mol cm^{-2}. All points corresponding to the CE-curve satisfy the condition $\tilde{\psi}(0) \geq 1$. The SA-curves represent the results obtained by using eqs. (21) and (22). For very large pores f approaches the FP-limit. It can be concluded from Fig. 3 that only for relatively small pore sizes (roughly for $a < 10^{-6}$ cm) a significant effect of the pore radius appears, a result already emerging from Fig. 1. In addition it can be seen that f decreases with increasing value of N.

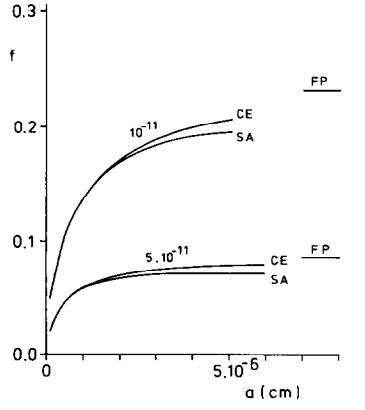

Fig. 3. Dependence of f on the pore radius for two values of N, $N = 10^{-11}$ mol cm^{-2} and 5×10^{-11} mol cm^{-2}. $\varepsilon = 78$; $T = 298$ K; $c = 10^{-7}$ mol cm^{-3} (1:1 electrolyte); pH = 5.7; $K_a = 10^{-8}$ mol cm^{-3}. CE: eqs. (20); SA: eqs. (21) and (22); FP: eq. (17).

An increase of the effective fixed charge concentration with the electrolyte concentration was experimentally observed by Tsimboukis et al. [4] in their study of the partition equilibria of Na^+ and Cl^- between cellulose membranes and aqueous NaCl-solutions at pH = 5.8 and $T = 295$ K. Cellulose membranes contain weakly ionizing carboxyl groups and therefore the experimental data seem quite suitable for an analysis on the basis of a simple dissociation equilibrium.

For the carboxyl group content of the membranes a value of 2.51×10^{-5} mol/(cm^3 pore volume) was reported [4]. Furthermore the authors were able to also estimate a mean pore radius, a of 6×10^{-7} cm, which is, as they mentioned, in reasonable agreement with an earlier reported result ($a = 4.8 \times 10^{-7}$ cm). Using the former value we calculate (see eq. 27) that $N = 7.53 \times 10^{-12}$ mol cm^{-2}, from $2N/a = 2.51 \times 10^{-5}$ mol cm^{-3}. Tsimboukis et al. [4] added to several membranes Direct Blue 1 which enlarges the fixed charge concentration by strongly ionizing SO_3H-groups. The dye content was determined spectrophotometrically. Here we analyse the results (Fig. 2 of ref. [4]) for a dyeless membrane and two membranes with dye contents corresponding to SO_3^--surface concentrations of respectively 5.73×10^{-12} mol cm^{-2} and 1.31×10^{-11} mol cm^{-2}. Also these values for $[SO_3^-]$ were calculated by assuming a pore radius equal to 6×10^{-7} cm. The maximum value of α, which corresponds to the membrane with the highest dye content ($[SO_3^-] = 1.31 \times 10^{-11}$ mol cm^{-2}) and whose carboxyl groups are completely ionized ($[A^-] = N = 7.53 \times 10^{-12}$ mol cm^{-2}), equals 1.7. Therefore the SA-expressions may be considered as a good approximation for the membrane systems which are discussed here.

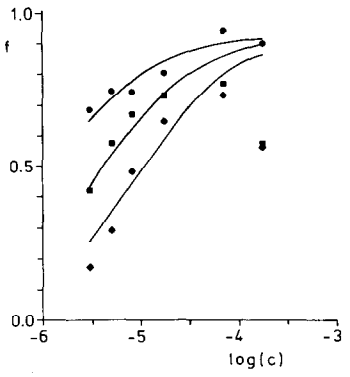

Fig. 4. Concentration dependence of the fraction (f) of carboxyl groups which are actually ionized, experimentally observed with cellulose membranes and NaCl-solutions (T = 295 K, pH = 5.8, carboxyl group content 2.51×10^{-5} mol/cm^3 pore volume) [4]. Measuring points fitted with SA-curves: eqs. (21) and (22). $\varepsilon = 78$; $a = 6 \times 10^{-7}$ cm; $N = 7.53 \times 10^{-12}$ mol cm^{-2}; $K_a = 2.3 \times 10^{-8}$ mol cm^{-3}. [SO_3^-]: 0 mol cm^{-2} (●), 5.73×10^{-12} mol cm^{-2} (■) and 1.31×10^{-11} mol cm^{-2} (◆).

Hence in all calculations eqs. (21) and (22) were used. With preset values $N = 7.53 \times 10^{-12}$ mol cm^{-2} and $a = 6 \times 10^{-7}$ cm, the acid constant (K_a) was varied in order to fit the theoretical curve to the experimental points obtained with the "dyeless" membrane. In this way we found $K_a = (2.3 \pm 0.2) \times 10^{-8}$ mol cm^{-3}. Using $N = 7.53 \times 10^{-12}$ mol cm^{-2}, $a = 6 \times 10^{-7}$ cm and $K_a = 2.3 \times 10^{-8}$ mol cm^{-3} also theoretical curves for the stained membranes were calculated. These curves fit the experimental data reasonably, as can be seen in Fig. 4. The experimental points corresponding to the highest concentration ($c = 1.72 \times 10^{-4}$ mol cm^{-3}) deviate from the expected behaviour because the experimental error was largest at this concentration [4] (see also Fig. 2 of ref. [4]).

It is interesting to note that the fraction of carboxyl groups which are actually ionized decreases with increasing dye content. This can easily be understood considering that the absolute value of the wall potential increases with increasing surface concentration of SO_3^--groups which results in a shift of the equilibrium $AH \rightleftarrows A^- + H^+$ to the left.

Assuming $a = 6 \times 10^{-7}$ cm our analysis leads to $K_a = (2.3 \pm 0.2) \times 10^{-8}$ mol cm^{-3}, a value which is acceptable for carboxyl groups. Using the other value of the pore radius, $a = 4.8 \times 10^{-7}$ cm, we obtained along the same route $K_a = (2.0 \pm 0.2) \times 10^{-8}$ mol cm^{-3} and reasonable fits for all three membranes. Because the pore radius is an uncertain factor we followed also another procedure. Assuming $K_a = 1.8 \times 10^{-8}$ mol cm^{-3}, the acid constant of the carboxyl group of acetic acid, the pore radius was varied at constant ratio $2N/a = 2.51 \times 10^{-5}$ mol cm^{-3} in order to perform the curve fitting for the "dyeless" membrane. The curve is not very sensitive to the pore radius since we found $a = (4 \pm 2) \times 10^{-7}$ cm. This at least indicates that we are dealing here with fine porous membrane systems which is in agreement with the pore radii mentioned before.

We also applied the site dissociation model to experimental results of Koh et al. [6] obtained with mica track-etched membranes. These membranes have a well-defined pore structure in which probably weakly ionizing silanol (SiOH) groups are present. Using the space-charge model the authors analysed KCl-conductivity data. Here we only discuss the results obtained at pH 7 for the membrane with $a = 1.20 \times 10^{-6}$ cm which contained no heparin.

It was found (see Table 2 of ref. [6]) that q^* strongly increases with increasing KCl-concentration. According to our analysis in terms of the site dissociation model some discrepancy between theory and experiment remains to exist. On the ground of KCl-conductivity findings Westermann–Clark et al. [7] suggested that in the case of mica track-etched membranes Cl^--ions may strongly adsorb onto the pore wall. Indeed the discrepancy observed by us can be ascribed to the occurrence of coion adsorption. We conclude that with mica track-etched membranes both weakly ionizing acid groups and coion adsorption are involved in the observed increase of q^* with the KCl-concentration.

When weakly acid groups are attached on the capillary wall the effective charge density also depends on the pH of the external solution. In fact the study of the pH dependence of q^* provides an excellent means to trace the presence of these groups.

The variation of f with the pH at constant electrolyte concentration ($c = 10^{-6}$ mol cm^{-3}) is shown in Fig. 5. For K_a two values are consid-

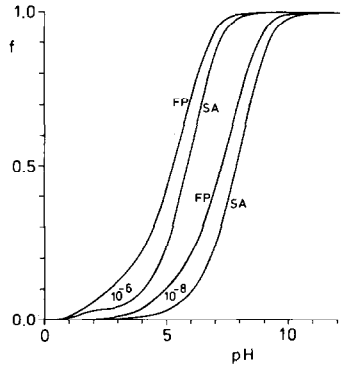

Fig. 5. Dependence of f on the pH for two K_a-values, $K_a = 10^{-8}$ and 10^{-6} mol cm^{-3}. $\varepsilon = 78$; $T = 298$ K; $c = 10^{-6}$ mol cm^{-3} (1:1 electrolyte); $N = 5 \times 10^{-11}$ mol cm^{-2}; FP = curve: eq. (17); SA-curve ($a = 10^{-7}$ cm): eqs. (21) and (22).

ered, 10^{-8} mol cm^{-3} and 10^{-6} mol cm^{-3}. In the calculation of the SA-curves a pore radius of 10^{-7} cm has been taken. The curves possess the characteristic S-shape which remains the same also when other values of the parameters N, K_a and c are assumed. The FP-curves are already known from literature [1,3]. Here too the influence of the pore radius can be observed.

In their experiments on track-etched mica membranes Westermann–Clark et al. [7] observed that the effective charge density strongly varied from zero to a pH-independent negative value when the pH was increased from 4.5 to 7 at constant KCl-concentration ($c = 10^{-5}$ mol cm^{-3}; Fig. 2 or ref. [7]). This result, which is in agreement with our theoretical findings (Fig. 5), indicates the presence of weakly ionizing silanol groups ($SiOH \rightleftarrows SiO^- + H^+$). Within this context it is interesting to note that the authors also found positive values for the effective charge density in the range pH < 4.5 which may indicate the amphiprotic character of a silanol group ($SiOH + H^+ \rightleftarrows SiOH_2^+$). We carried out computer simulations for the case in which amphoteric groups are present and found indeed curves having the same features for the whole pH-range as the curve shown in Fig. 2 of ref. [7].

Finally we discuss the experimental results obtained by Demisch and Pusch with an asymmetric cellulose acetate membrane and NaCl-solutions [5]. They measured the electro-osmotic permeability (l_{ep}), the filtration coefficient (L_p) and the electrical resistance (R_e). The experimental conditions were $T = 298$ K, pH = 5.8 and $c = 2 \times 10^{-5}$ mol cm^{-3}. From titration data a carboxyl group content ($2N/a$) of 5.0×10^{-6} mol/(cm^3 pore volume) was found.

Using Donnan's theory in which the value of a is irrelevant the above authors [5] calculated the effective fixed charge concentration from the experimentally determined value of $l_{ep}/L_p R_e$ by applying eq. (28) and discussed the result in the light of a simple dissociation equilibrium of weakly acid groups. They obtained semiquantitative agreement between the experimental findings and the theoretical results. Here we try to improve the above agreement by taking into account the effect of the pore radius.

The first step in our analysis is the estimation of q^* from the quantity $l_{ep}/L_p R_e$ by applying the space-charge model for various values of the pore radius. For the a-values listed in Table 1 first $\tilde{\psi}_w - \bar{\tilde{\psi}}$ (column 2) was calculated from the experimental value of $l_{ep}/L_p R_e$ by means of eqs. (23) and (24). Then applying the SA-solution (eqs. 11 and 12) of the PB-equation, which is permitted since $\tilde{\psi}_w - \bar{\tilde{\psi}} < 1$, we obtained the corresponding values for q^* (column 3) and $\tilde{\psi}_w$ (column 4). It can be seen from Table 1 that q^* increases when a larger pore radius is assumed. For $a = 10^{-7}$ cm

Table 1
The dependence of f on a as it follows from the experimental value of $l_{ep}/L_p R_e$ obtained by Demisch and Pusch [5] with an asymmetric cellulose acetate membrane ($T = 298$ K, pH 5.8, $c = 2 \times 10^{-5}$ mol cm^{-3}; $l_{ep}/L_p R_e = 6.16 \times 10^8$ e.s.u. cm^{-3}; carboxyl group content 5×10^{-6}/cm^3 pore volume). Intermediate results are shown in the various columns

$a \times 10^7$ (cm)	$\tilde{\psi}_w - \bar{\tilde{\psi}}$	q^* (e.s.u. cm^{-2}) [a]	$\tilde{\psi}_w$	$N \times 10^{12}$ (mol cm^{-2})	f
1	0.001	31	0.055	0.25	0.43
5	0.036	186	0.101	1.25	0.51
10	0.145	513	0.233	2.50	0.71
11	0.175	601	0.270	2.75	0.76
12	0.209	695	0.309	3.00	0.80
13	0.245	795	0.350	3.25	0.85
14	0.284	905	0.396	3.50	0.89
15	0.326	1020	0.443	3.75	0.94
20	0.580	1710	0.727	5.00	1.18

[a] 1 e.s.u. = 3.333×10^{-10} C.

the q^*-value in Table 1 agrees with the result obtained by using the Schmid equation (eq. 28).

At each value of the pore radius N (column 5) is known ($2N/a = 5.0 \times 10^{-6}$ mol cm^{-3}) and therefore also f (column 6) can be calculated. The value of f exceeds unity for pore radii roughly larger than 2×10^{-6} cm and consequently these values of a cannot be considered as realistic.

In the next step of the analysis we consider the dissociation of the carboxyl groups. Assuming an acceptable value for K_a, i.e. $K_a = 1.8 \times 10^{-8}$ mol cm^{-3}, we have pH $-$ p$K_a = 1.06$. The values of $\tilde{\psi}_w$ listed in Table 1 are rather small and therefore it is acceptable to neglect as a first approximation $\tilde{\psi}_w/2.303$ in eq. (15) with respect to this value of pH $-$ pK_a. This implies that the maximum value of f at pH 5.8 is approached, i.e. $f \approx 0.92$. Using the N-values given in Table 1 and assuming $K_a = 1.8 \times 10^{-8}$ mol cm^{-3} we also carried out a more accurate calculation using eqs. (21) and (22) and found that f varied only from 0.91 to 0.87 when the pore radius is increased from 10^{-7} cm to 2×10^{-6} cm. Taking a global spreading for f from 0.85 to 0.95 we find that the found value for $l_{ep}/L_p R_e$ is consistent with a ranging from 1.3×10^{-6} cm–1.5×10^{-6} cm. Furthermore our analysis indicates that at pH = 5.8 and $c = 2 \times 10^{-5}$ mol cm^{-3} roughly 90% of the carboxyl groups are ionized.

An implication which arises with asymmetric cellulose acetate membranes is that the dielectric constant of the solution in ultrafine pores may be considerably smaller than its free solution value. Taking $\varepsilon = 4$ instead of $\varepsilon = 78$ we repeated the calculation and found another range for a, being 3×10^{-7} cm–4×10^{-7} cm, and the same value for f, $f \approx 0.9$. Thus the value of the pore radius obtained in our analysis is rather sensitive to the choice of ε. A lower dielectric constant yields a smaller pore radius. The estimated value of f, however, remains about 0.9 which in any way indicates that we are dealing with small values of $\tilde{\psi}_w$ or $\tilde{\psi}_w/2.303 \ll$ pH $-$ pK_a.

Another aspect of an asymmetric cellulose acetate membrane which cannot be left undiscussed is the asymmetric structure, consisting globally of a selective layer, in which the pore size gradually increases from ultrafine at the top of the membrane to moderate, and a highly porous layer in which free solution properties may be assumed. As a result of this asymmetry a volume flow may cause internal concentration polarization. The linear relationship between streaming potential and applied pressure difference observed by Demisch and Pusch, however, indicates that the effect of internal concentration polarization on the experimental result is negligible. We may therefore assume that the forces and resulting flows through the membrane in the above experiment were relatively small. At relatively small forces and flows the measured transport coefficients reflect average properties of the whole membrane and therefore the pore radius obtained in our analysis, a in the range 1.3×10^{-6} cm–1.5×10^{-6} cm, can only have the meaning of a structure-averaged radius.

4. Conclusion

Charge formation in microporous charged membranes can reasonably be understood by modelling the PB-equation in a simple surface dissociation equilibrium. At small values of the pore radius only solutions of the PB-equation can be used which also account for the curvature of the pore surface. Agreement between theory and experiment is expected to be found and is found in reality when ionization of the functional groups in the only mechanism. Obviously the model ought to be extended when other effects as sorption of counterions and coions are observed. In the case of cellulose membranes, whose properties are adequately described by the single (acid) site model, the characteristic pK_a of carboxyl groups is found.

References

1 Robert J. Hunter, Zeta potential in colloid science "principles and applications" (Academic Press, New York, NY, 1981).
2 J.N. Israelachvili, Intermolecular and surface forces (Academic Press, New York, NY, 1985).
3 Thomas H. Healy and Lee R. White, Ionizable surface group models of aqueous interfaces, Adv. Colloid Interface Sci. 9 (1978) 303.

4 D.G. Tsimboukis and J.H. Petropoulos, Behaviour of simple ions in the system cellulose-anionic dye-simple electrolyte. Part 1-partition equilibria, J. Chem. Soc., Faraday Trans. 1, 75 (1979) 705.
5 H.U. Demisch and W. Pusch, Ion exchange capacity of cellulose acetate membranes, J. Electrochem. Soc.: Electrochem. Sci. Technol. 123 (3) (1976) 370.
6 Wei-Hu Koh and John L. Anderson, Electroosmosis and electrolyte conductance in charged microcapillaries, AIChE J. 21 (6) (1975) 1176.
7 G.B. Westermann-Clark and J.L. Anderson, Experimental verification of the space-charge model for electrokinetics in charged microporous membranes, J. Electrochem. Soc.: Electrochem. Sci. Technol. 130 (4) (1983) 839.
8 H.J.M. Hijnen, J. van Daalen and J.A.M. Smit, The application of the space-charge model to the permeability properties of charged microporous membranes, J. Colloid Interface Sci. 107 (2) (1985) 525.
9 J.A.M. Smit, Reverse osmosis in charged membranes: analytical predictions from the Space-charge model, J. Colloid Interface Sci. 132 (2) (1989) 413.
10 E. Hawkins Cwirko and R.G. Carbonell, Transport of electrolytes in charged pores: analysis using the method of spatial averaging, J. Colloid Interface Sci. 129 (2) (1989) 513.
11 H. van Keulen and J.A.M. Smit, submitted for publication to the J. Colloid Interface Sci. (1991).